

Proteasome and thiol involvement in quality control of glycosylphosphatidylinositol anchor addition

Barry WILBOURN¹, Darren N. NESBETH¹, Linda J. WAINWRIGHT^{1,2} and Mark C. FIELD³

Laboratory of Cell Biology, Department of Biochemistry, Imperial College of Science, Technology and Medicine, London SW7 2AY, U.K.

Improperly processed secretory proteins are degraded by a hydrolytic system that is associated with the endoplasmic reticulum (ER) and appears to involve re-export of luminal proteins into the cytoplasm for ultimate degradation by the proteasome. The chimaeric protein hGHDAF28, which contains a crippled glycosylphosphatidylinositol (GPI) C-terminal signal peptide, is degraded by a pathway highly similar to that for other ER-retained proteins and is characterized by formation of disulphide-linked aggregates, failure to reach the Golgi complex and intracellular degradation with a half life of ~ 2 h. Here we show that *N*-acetyl-leucinal-leucinal-norleucinal, MG-132 and lactacystin, all inhibitors of the proteasome, protect hGHDAF28; hGHDAF28 is still proteolytically cleaved in the presence of lactacystin or MG-132, by the removal of ~ 2 kDa, but the truncated fragment is not processed further. We demonstrate that the ubiquitination system accelerates ER-degradation of

hGHDAF28, but is not essential to the process. Overall, these findings indicate that GPI quality control is mediated by the cytoplasmic proteasome. We also show that the presence of a cysteine residue in the GPI signal of hGHDAF28 is required for retention and degradation, as mutation of this residue to serine results in secretion of the fusion protein, implicating thiol-mediated retention as a mechanism for quality control of some GPI signals. Removal of the cysteine also prevents inclusion of hGHDAF28 in disulphide-linked aggregates, indicating that aggregate formation is an additional retention mechanism for this class of protein. Therefore our data suggest that an unpaired terminal cysteine is the retention motif of the hGHDAF28 GPI-processing signal and that additional information may be required for efficient engagement of ER quality control systems by the majority of GPI signals which lack cysteine residues.

INTRODUCTION

Quality control of post-translational modification is an important facet of protein synthesis. For secretory and cell surface proteins such control is frequently mediated by selective retention and degradation by the endoplasmic reticulum (ER) [1–3]. Recently, details of this ER-associated degradation (ERAD) pathway have been elucidated [4,5]. ERAD substrate proteins are re-exported to the cytosol, probably via the sec61p pore complex, and disposed of by the ubiquitin/proteasome system [5–7]. Glycopeptides and oligosaccharides are released from the ER in an ATP- and, in the case of glycopeptides, cytosol-dependent manner [8–10]. ERAD substrate forms of carboxypeptidase Y, α -factor and human α -1-proteinase inhibitor are released from yeast microsomes *in vitro* [11,12], suggesting a similar mechanism for peptides and proteins, and ERAD mutants have identified proteasome subunits and components of the ubiquitination system [12,13].

In mammalian cells the ubiquitination system is part of the ERAD pathway [14–16], and most ERAD substrates are stabilized by the protease inhibitors *N*-acetyl-leucinal-leucinal-norleucinal (ALLN) and lactacystin, the latter being more specific for the proteasome [17–19]. MHC class I chains are translocated to the cytosol via the sec61p pore in cells expressing the cytomegalovirus US2 protein [20], whereas in normal cells misfolded class I chains are exported and degraded by a lactacystin-

sensitive process [21]. For a subset of substrates the ubiquitin pathway appears to be dispensable to the ERAD process [22].

The glycosylphosphatidylinositol (GPI) anchor, a complex glycolipid, is the mechanism of cell membrane attachment for many proteins [23,24]. GPI attachment requires translocation of the polypeptide across the ER membrane, presumably via the sec61p pore, followed by cleavage of a C-terminal signal between two small side-chain amino acids 10–12 residues N-terminal of the hydrophobic domain [25,26], and its replacement, in a coupled process, by preformed GPI lipid. The protein is then transported through the Golgi apparatus to the cell surface. GPI signals conform to a canonical structure: the C-terminus of the nascent chain is hydrophobic, ~ 15 amino acids in length, with a spacer region of 10–15 residues N-terminal of this [24]; a similar architecture is found in the C-terminus of the α - and β -subunits of the T-cell receptor, both of which are ERAD substrates [22,27]. Recent evidence suggests involvement of the proteasome in GPI quality control by lactacystin inhibition [28].

When GPI addition is prevented by mutation of the cleavage site, instead of rapid export to the cell surface the protein fails to be included into ER transport vesicles and is retained [28–30]. Degradation, by a non-lysosomal mechanism, is rapid and has the features of ERAD [31–33]. We have been studying the fate of a chimaeric protein, hGHDAF28, which is made from the entire human growth hormone (hGH) sequence, fused to the GPI signal of decay accelerating factor (DAF). hGHDAF28 contains

Abbreviations used: ALLM, *N*-acetyl-leucinal-leucinal-methioninal; ALLN, *N*-acetyl-leucinal-leucinal-norleucinal; CHO, Chinese hamster ovary; DAF, decay accelerating factor; DCI, 3,4-dichloroisocoumarin; DTT, dithiothreitol; ER, endoplasmic reticulum; ERAD, endoplasmic reticulum-associated degradation; GPI, glycosylphosphatidylinositol; hGH, human growth hormone; LB, Luria-Bertani.

¹ These authors contributed equally to the experimental work reported in this paper.

² Present address: Divisione di Oncologia Pediatrica, Università Cattolica del Sacro Cuore, Largo A. Gemelli 8-00168 Roma, Italia.

³ To whom correspondence should be addressed (e-mail m.field@ic.ac.uk).

a crippled version of the DAF GPI-signal (see Table 2 for a description of the constructs), due to a point mutation at the processing site [29,32]. hGH itself is a non-glycosylated protein monomer containing 191 amino acids and two disulphide bridges, between cysteine residues 53 and 165 and 182 and 189 respectively. Close proximity of the C-terminal disulphide bond to a cysteine at position 203 within the DAF GPI-signal is suggestive of disulphide shuffling between residues 182, 189 and 203 to create intermolecular cross-links.

In this paper we investigate in detail the role that cytoplasmic components play in hGHDAF28 degradation and the effect of manipulations of the GPI signal itself. Our data indicate that hGHDAF28 is indeed exported from the ER for proteasomal degradation and that retention is critically dependent on the presence of a cysteine residue within the GPI signal.

MATERIALS AND METHODS

Nucleic acids

Construction of the expression vector pRK5·hGHDAF28 has been described previously [33]. Other forms of hGHDAF were constructed as follows. The *EcoRI* fragment containing the hGHDAF28 minigene from hGHDAF28·pRK5 was subcloned into pSG5 to produce pKRS·28. Specific mutations of the C-terminal sequence were generated by oligonucleotide-directed mutagenesis of pKRS·28 (see below). Oligonucleotides were synthesized by Genosys Plc. U.K. PCR fragments, consisting of a given mutated region, were then transferred into vector plasmid using standard DNA manipulations. Plasmids were purified from *Escherichia coli* XL1-Blue or DH5 α cell cultures with the Qiagen Midi Kit. Immunogen International Mini Preps were used for small-scale purifications. Linear plasmid or PCR fragments were purified from agarose gels with the GeneClean Kit (Bio 101). All kits were used according to manufacturers' directions. Restriction digests were performed using enzymes from MBI Fermentas or New England Biolabs, Inc. PCR was carried out using standard procedures [34] on a Perkin-Elmer 480 Thermal Cycler with Taq polymerase to generate mutant sequences. Reaction volumes of 50 μ l typically consisted of 1 μ l (2.5 units) of Taq polymerase, 250 μ M dNTPs, 5 mM MgCl₂, reaction buffer [16 mM (NH₄)₂SO₄/67 mM Tris/HCl, pH 8.8, at 25 °C/0.01% (v/v) Tween 20], 2 ng of template DNA and 0.2 μ mol of each primer. Primer sequences are given below. The denaturation step was at 94 °C for 60 s. Annealing was achieved at 68–70 °C, depending on primer T_m, for 2 min and extensions were at 72 °C for 3 min. Thirty cycles were used.

Ligations were performed with 1 Weiss unit of T4 ligase in the presence of a reducing buffer [66 mM Tris/HCl (pH 7.5 at 25 °C), 5 mM MgCl₂, 10 mM dithiothreitol (DTT) and an ATP solution (1 mM ATP in 5 mM Tris/HCl, pH 7.5)] in a total volume of 20 μ l. Ligation reactions were incubated overnight at 14 °C.

Bacterial transformations were achieved by electroporation with a BTX ECM600 electroporator: 2.5 kV HV mode, 720 Ω resistance, 2 mm chamber gap, 1.25 kV charging voltage, 6.25 kV cm⁻¹ desired field strength and 5 ms desired pulse length. Competent cells (100 μ l) were mixed with 2 μ l of ligation reaction before electroporation. These cells were then resuspended in 1 ml of Luria-Bertani (LB) broth, placed in a shaker at 37 °C for 30 min and then spread on an LB agar plate containing ampicillin. This plate was incubated overnight at 37 °C. Any resultant colonies were transferred into 1 ml of LB broth with ampicillin and incubated in a shaker at 37 °C overnight. All DNA fragments were separated using agarose gel electrophoresis, visualized with

ethidium bromide staining and their sizes assessed with a 1 kb molecular mass ladder (Gibco-BRL).

hGHDAF28·KDEL and hGHDAF28·R4 were produced with forward and reverse primers (5'Bgl: GGACTGGGCAG-ATCTTCAAGC and KDELoligo: GGGATATCTTATCTA-CAGCTCGTCTTAGTCAGCAAGCC or R4oligo: GG-GATATCTTATCTACCTCCTCCTCCTAGTCAGCAAGCC respectively) containing the appropriate codon insertions (bold) and deletion of an *XmaI* restriction site. This deletion allowed ligation of the PCR fragment into pKRS·28 to be confirmed by restriction analysis. New plasmids, pKRS·KDEL and pKRS·R4, were thus generated encoding hGHDAF28·KDEL and hGHDAF28·R4 respectively. hGHDAF28·C203S was generated with pKRS.28 as template using C203SFor: GGT-ACTACGCGTCTTCTATCTGGGCACACGTCTTTCACG-TTG as forward primer (nucleotide substitutions in bold) and BsmOligo: ACAAAACCACATCTAGAATGCAGTG, a reverse primer containing no restriction-site alterations. Ligation of the resultant PCR fragment into pKRS·KDEL introduced an *XmaI* site. All ligations were directional and constructs were verified by sequence determination (both strands) for the mutagenized region. After expression, small alterations in migration of the KDEL and R4 products on SDS/PAGE were clearly visible.

Chemicals and antibodies

Cleland's reagent (DTT), Nonidet P40, Triton X-100, Protein A-Sepharose, leupeptin, chymostatin, antipain, pepstatin A, trypsin, *N*-acetyl-leucinal-leucinal-methioninal (ALLM), ALLN, EDTA, EGTA, PMSF and 7-amino-1-chloro-3-L-tosylamidoheptan-2-one (TLCK) were all from Sigma. Pansorbin, E64, 3,4-dichloroisocoumarin (DCI), lactacystin and MG-132 were purchased from Calbiochem. Compounds for addition to living cells were made up in PBS, tissue culture grade DMSO (Sigma) or ethanol at a concentration such that the final volume added did not exceed 20 μ l/ml. Polyclonal antisera to recombinant hGH were raised in rabbits or mice using RIBI[®] as adjuvant (Sigma).

Transfections

COS7 or Chinese hamster ovary (CHO) cells were cultured in Dulbecco's modified Eagle's medium or alpha-minimal essential medium respectively, containing 10% (v/v) heat-inactivated foetal calf serum plus 2 mM L-glutamine, 5 units/ml penicillin and 5 mg/ml streptomycin (all from Sigma) in a 5% CO₂ atmosphere at 37 °C. Cells were transfected using Lipofectamine[®] (Gibco-BRL) as described [33]. Wild-type (K1) cells were grown at 37 °C, whereas the E36 and ts20 cells were maintained at 30 °C. Stable CHO cell lines expressing hGHDAF mutants were produced by a double transfection with the relevant hGHDAF construct and pcDNA3, which contains the neomycin selectable marker, at a molar ratio of 10:1. Cells were allowed to recover from the transformation for 72 h and were then selected with neomycin. After 2 weeks transformants were checked for expression of the transgene by immunofluorescence.

Metabolic labelling and immunoprecipitation

Cells were metabolically labelled by starving in methionine/cysteine-free minimum essential medium (Gibco-BRL) with [³⁵S]methionine (Amersham) at ~ 75 μ Ci/35 mm dish. Cells were harvested, detached from the substrate, lysed and immunoprecipitated with lapine polyclonal anti-hGH as described [33]. Protein secreted into the medium was immunoprecipitated by harvesting the medium (1 ml), adding 12 μ l of 10% (v/v) SDS, 50 μ l of 20% (v/v) Nonidet P-40, 12 μ l of 0.5 M EDTA and

general protease inhibitors [33] and treating exactly as the cell extracts.

Protease inhibitors were used at the following concentrations: ALLM and ALLN, 100 $\mu\text{g/ml}$; DCI, 10 μM ; EDTA, 10 mM; EGTA and PMSF, 1 mM; pepstatin A and antipain, 1 μM ; and lactacystin and MG-132, 20 μM . All inhibitors were added 1 h before metabolic labelling (which lasted 1 h) and cells were maintained in the presence of the compound throughout the experiment. Fresh PMSF was added before labelling and after every hour in the chase period. For analysis of the role of ubiquitin and induction of the ubiquitin-negative phenotype, ts20 cells [and the E36 parental line as control (both gifts from Dr Ger Strous, University of Utrecht, The Netherlands)] were shifted to 44 °C for 1 h to induce the ts phenotype, followed by metabolic labelling for 1 h at 42 °C. Cells were then chased at 42 °C before analysis by immunoprecipitation.

Gel electrophoresis

Immunoprecipitates were analysed in 15 or 17% SDS/polyacrylamide gels by addition of 50 μl of SDS-containing sample buffer directly to the Protein A beads, followed by heating to 95 °C. In cases where samples were to be reduced, DTT was added, to a concentration of 50 mM, before heating. After electrophoresis at 15 V/cm (constant voltage), gels were fixed in 20% (v/v) methanol/10% (v/v) acetic acid, impregnated with En³Hance (NEN Dupont) and dried. The gels were then exposed to AR-XOMat film (Kodak) at -85 °C. Bands were quantified using a Phosphorimager system (Molecular Dynamics Inc.) or by scanning, followed by densitometry using NIH Image software on an APUS 3000/200 MacOS computer.

RESULTS

Degradation of hGHDAF28 is inhibited by the synthetic peptide ALLN

In order to gain some insight into the mechanism by which hGHDAF28 is degraded we tested recognized inhibitors of the four major classes of proteases (aspartyl, serine, cysteinyl and metallo) for their effect on hGHDAF28 stability. Transfected

Table 1 Stabilization of hGHDAF28 by ALLN, lactacystin and MG-132

Data are expressed as the degradative index (DI) of hGHDAF28 after a chase of 3 h. DI is calculated as $[\text{counts}_{t=0\text{ h}} - \text{counts}_{t=3\text{ h}}]_{\text{treated}} / [\text{counts}_{t=0\text{ h}} - \text{counts}_{t=3\text{ h}}]_{\text{control}}$. Cells were pretreated with the compounds for 1 h before pulse-labelling. Experiments were done three times, except for ALLN (experiment done eight times) and MG-132 (four times) and S.D.s are indicated. The control, DI = 1.0, routinely had S.D. = ± 0.12 . All analyses were performed in transiently transfected COS cells, except for the lactacystin and MG-132 experiments, where stably transfected CHO cell lines were used. Concentrations of the various compounds used are described in the Materials and methods section.

Compound	D.I. (3 h)	S.D.
Antipain	1.03	0.08
PMSF	0.97	0.15
Pepstatin A	1.03	0.17
EDTA	0.90	0.05
E64	1.00	0.18
EGTA	1.12	0.15
DCI	1.05	0.07
ALLM	0.87	0.07
ALLN	0.66	0.07
MG132	0.25	0.06
Lactacystin	0.18	0.02

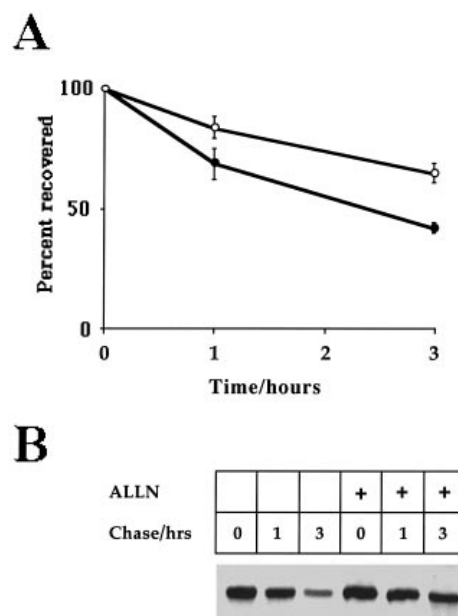


Figure 1 The cysteine protease inhibitor ALLN decreases the rate of hGHDAF28 degradation

(A) Cells expressing hGHDAF28 were pretreated for 1 h with 100 $\mu\text{g/ml}$ ALLN, pulse-labelled for 1 h and chased. The amount of hGHDAF28 was quantified by immunoprecipitation and SDS/PAGE analysis under reducing conditions, followed by visualization by Phosphorimager (\bullet , control; \circ , 100 $\mu\text{g/ml}$ ALLN-treated). The experiment was done four times with the S.D.s indicated. (B) Autoradiograph of reduced SDS/PAGE analysis of hGHDAF28 immunoprecipitates from ALLN-treated (+) and control COS cells. Note the presence of a faint lower-molecular-mass band in the rightmost lane.

COS-7 cells were pretreated with the various protease inhibitors for 1 h and maintained during the rest of the experiment (Table 1). After immunoprecipitation and resolution by SDS/PAGE we quantified the amount of hGHDAF28 remaining after a 3 h chase. No significant effects were observed with serine protease inhibitors (DCI and PMSF), an aspartic protease inhibitor (pepstatin), the metalloprotease inhibitors (EDTA and EGTA) or a mixed specificity inhibitor of both serine and cysteine proteases (antipain). This suggests that proteases of the serine, aspartic or metallo classes are not required for ERAD of hGHDAF28.

We subsequently tested several specific cysteine protease inhibitors. The synthetic tetrapeptide ALLN significantly blocked degradation of hGHDAF28 (Table 1). ALLN inhibits the activity of calpains (specifically class I), cathepsins L and B as well as proteasomal activities [35]. In contrast, ALLM and E64, also cysteine protease inhibitors, but with little effect on the proteasome, had no significant effect on the stability of hGHDAF28 (Table 1). We examined the kinetic effect of ALLN, which confirmed inhibition of hGHDAF28 degradation and that the effect was prolonged (Figure 1). We also observed a small amount of an additional band at later time points, suggesting that a processing intermediate had been detected (Figure 1B, last lane). These data indicate that hGHDAF28 turnover requires an ALLN-sensitive, ALLM-resistant, cysteine protease, possibly the β -subunits of the 26S proteasome.

Degradation of hGHDAF28 requires the proteasome

In order to increase the accuracy, reproducibility and ease of our analysis we created three stable CHO cell lines. These expressed

Table 2 Constructs and residues discussed in this paper

hGHDAF29 represents the parent construct from which the others are derived ([36] and this paper). The C-terminal GPI signal sequence is shown. The position of the GPI attachment site is indicated by ·; Cys-203, the last residue in the amphipathic spacer region, is underlined.

hGH-EGSCGF^S·GTT^RLLSGHT^CFTL^TGLLGLT^LVTMGLLT

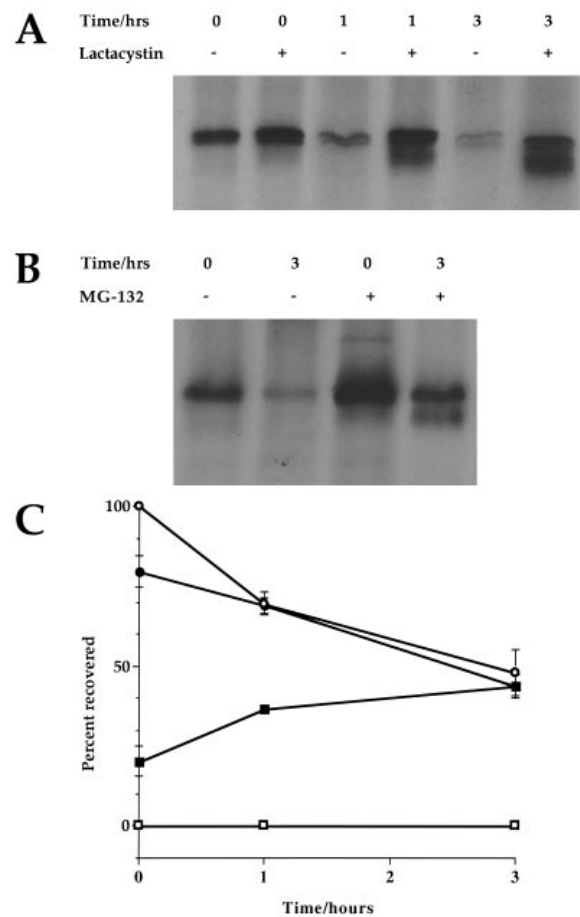
Construct	Alterations from hGHDAF29	Reference
hGHDAF29	None	[36]
hGHDAF28	Deletion of Ser-192. GPI-signal non-functional	[36]
hGHDAF28·KDEL	Addition of tetrapeptide sequence KDEL to C-terminus	This paper
hGHDAF28·R4	Addition of tetrapeptide sequence RRRR to C-terminus	This paper
hGHDAF28·C203S	Mutagenesis of Cys-203 to Ser-203	This paper

hGHDAF28, hGHDAF29 and hGHDAF28·KDEL (see Table 2). In some of our earlier experiments the transient transfection protocol has proven to have significant variability, necessitating a large number of replicates. We tested the effects of the proteasome inhibitors lactacystin and MG-132 on hGHDAF28 stability. The results for both compounds were very similar. A dramatic increase in stability was observed (Table 1). On further analysis we observed that hGHDAF28 was rapidly cleaved into a lower-molecular-mass species, losing ~ 2 kDa, which we designated p24, the 24 kDa form (Figure 2) and, based on the molecular mass, probably corresponding to the truncated form seen with ALLN. This initial processing was lactacystin insensitive and was also unaffected by co-treatment of cells with ALLN, ALLM, antipain or pepstatin plus 20 µM lactacystin (results not shown). Therefore we were unable to ascribe a protease activity responsible for hGHDAF28 to p24 conversion.

Further processing of the fusion protein was almost undetectable, although in overnight incubations significant degradation was observed, partly accounted for by cell lysis (results not shown). Processing intermediates other than p24 were never seen, suggesting that subsequent lactacystin-sensitive processing was rapid, consistent with the concerted mode of action of the proteasome. This also explains why in uninhibited cells degradation intermediates for hGHDAF28 and other ERAD substrates are rarely seen [33]. Quantification confirmed that p24 was indeed a product of the full-length fusion protein, as p24 abundance increased at early times concomitant with loss of full-length hGHDAF28 (Figure 2C). In addition, the kinetics of conversion of hGHDAF28 into p24 closely paralleled the degradation of hGHDAF28 in untreated cells (cf. Figures 2 and 4). In our system the effects of MG-132 were not readily reversible, as degradation was still inhibited for several hours after a washout, which may reflect the presence of a retained intracellular pool of the inhibitor.

Involvement of ubiquitination in hGHDAF28 degradation

We next assessed the importance of the ubiquitination pathway, an important component of the proteasomal disposal system in ERAD of hGHDAF28, by making use of a CHO cell line (ts20), temperature-sensitive for the E1 enzyme of the ubiquitin pathway [14]. When hGHDAF28 was transiently expressed in a normal CHO cell line maintained at 42 °C the transgene product was rapidly degraded with a half-life of ~ 90 min, as determined from the plot shown in Figure 3. E36 cells, the ts20 parental line, heat shocked and then maintained at 42 °C, degraded hGHDAF28 with a rate indistinguishable from the wild-type CHO cell line. In contrast, when hGHDAF28 was expressed in

**Figure 2** Proteasomal inhibitors protect hGHDAF28 from degradation

CHO cells expressing hGHDAF28 were pretreated for 1 h with lactacystin or MG-132, metabolically labelled for 1 h and chased by addition of complete medium containing drug. The fate of hGHDAF28 was monitored by immunoprecipitation and SDS/PAGE. (A) Effect of lactacystin, showing the protection of hGHDAF28 and the appearance of a lower-molecular-mass form with time (p24). (B) Effect of MG-132. The behaviour of hGHDAF28 is similar to lactacystin-treated cells. Note that the recovery of antigen at $t = 0$ is greater in the drug-treated cells than in the controls; this is due to protection of hGHDAF28 during the labelling period. (C) Quantification of the effect of lactacystin on hGHDAF28 showing product–precursor relationship for p24 and hGHDAF28. Data from three identical experiments are shown, together with the S.D.s indicated. Note that, on average, 50% of the hGHDAF28 is recovered from these cells at 3 h, but that there is some variation in individual experiments. In the example in (A) recovery at this time point was < 30%: ○, intact hGHDAF28; □, p24; ●, intact hGHDAF28 lactacystin-treated; ■, p24 lactacystin-treated.

the ts20 cells under identical conditions to the E36 line, the protein was significantly stabilized, with a half-life of approximately 4 h, although degradation still proceeded, albeit at a slower rate and no longer conforming to exponential kinetics. Therefore these data suggest that the ubiquitin pathway plays a role in rapid hGHDAF28 turnover but is not essential. Additionally, the presence of the p24 degradation product was never observed in transfected ts20 cells.

Effect of mutations on hGHDAF28 kinetics

We next turned to the question of which structural features of the GPI tail are important for retention and hence entry into the ERAD pathway (see Table 2 for constructs). As most GPI-anchored proteins that fail to become anchored are shunted into ERAD, we initially expected that the overall structure of the GPI

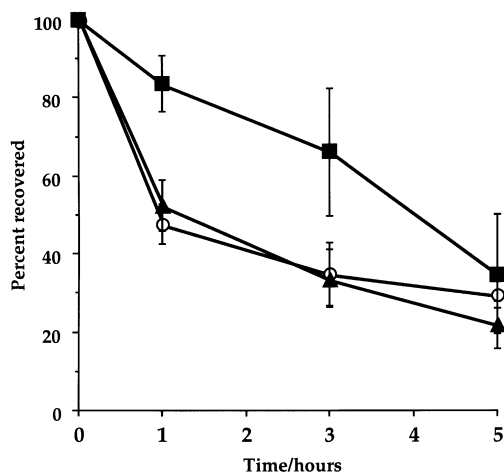


Figure 3 A functional ubiquitination system is required for efficient hGHDAF28 degradation

CHO cell lines expressing hGHDAF28 were pulse-labelled for 1 h and chased for the times shown. Degradation of hGHDAF28 was monitored by immunoprecipitation, SDS/PAGE and fluorography. Wild-type cells were maintained at 42 °C during the experiment, whereas E36 (parental) and ts20 cells were first heat-shocked to induce the ubiquitination defect as described in the Materials and methods section. Data are the means \pm S.D. of three experiments: ○, wild-type; ▲, E36; and ■, ts20 cells. At later time points the increased stability of hGHDAF28 in the ts20 cell line is lost (i.e. \geq 5 h), indicating the presence of a non-ubiquitin-dependent pathway.

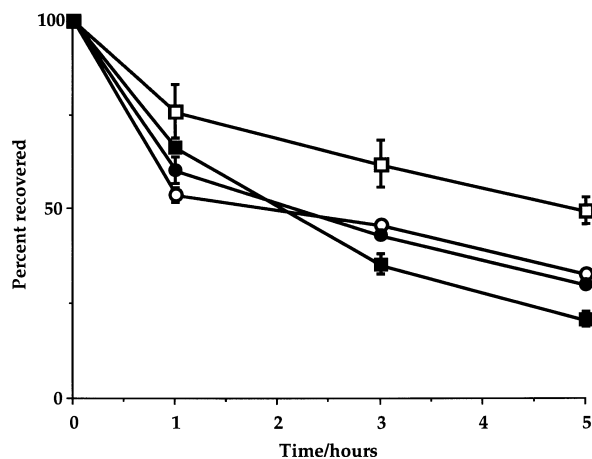


Figure 4 Effect of mutation of the C-terminus of hGHDAF28 on intracellular recovery

Pulse-chase analysis of the stability of various hGHDAF fusion proteins expressed in CHO cells. Cells were pulse-labelled for 1 h and chased for up to 5 h. Data are the means of two experiments: ○, hGHDAF28-KDEL; ■, hGHDAF28-R4; □, hGHDAF28-C203S; ●, hGHDAF28.

signal would be important. The similarity to the T-cell receptor α - and β -subunit C-termini has already been mentioned (above and [33]). In addition we have shown that the length of the spacer is important, since removal of the entire spacer, leaving the hydrophobic tail intact, allows secretion, whereas partial removal does not [32].

The tetrapeptide motif KDEL, which can cause the ER retrieval of normally non-ER-resident proteins when inserted into their amino acid sequence [37], was placed at the C-terminus

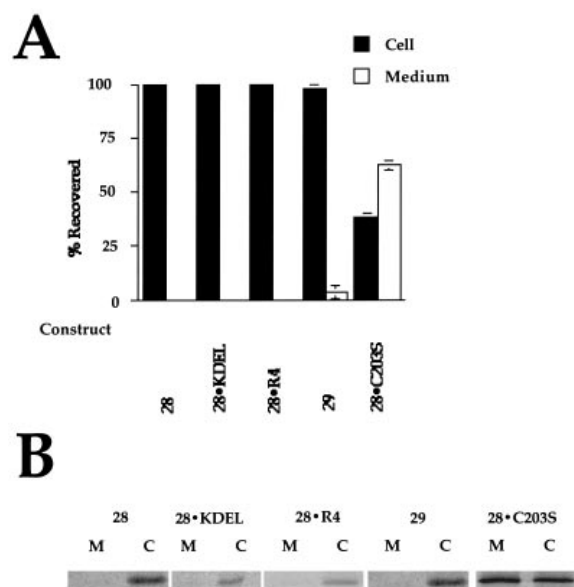


Figure 5 Mutation of Cys-203 in the C-terminus of hGHDAF28 leads to secretion

CHO cells expressing hGHDAF fusion proteins were pulse-labelled for 1 h. The medium was removed and replaced with complete medium and the cells were incubated for a further 3 h. After that time the cells and the media were harvested and analysed. (A) Quantification of immunoprecipitation data showing that hGHDAF28-C203S is secreted. Data are the means of two experiments. (B) Representative gel images used for quantification. Lanes: M, medium; C, cell lysate.

of hGHDAF28 to create hGHDAF28-KDEL. We also prepared a construct with four arginine residues at the C-terminus, hGHDAF28-R4, as an irrelevant control which has no known signal properties other than the potential to act as a stop-transfer signal in membrane anchorage. When analysed by expression in CHO cells, we found that the presence of KDEL or R4 had little effect on the stability of the fusion protein (Figure 4). In addition, by immunofluorescence microscopy the location of the proteins was found to be unchanged, retaining the reticular staining characteristic of an ER protein, and was not detected on the cell surface (results not shown). Therefore, the inclusion of a KDEL signal was not sufficient to prevent entry of hGHDAF28 into the ERAD pathway or to convert the protein into a transmembrane cell surface protein, as this latter situation would be predicted to allow expression of the fusion protein at the cell surface.

We next considered the role of the unpaired cysteine at position 203 (see Table 2). In λ -light-chains and IgM, a free C-terminal cysteine is important in mediating retention [38,39]. Much of our previous work has suggested that formation of aggregates is an important feature of the retention of hGHDAF28 [32,33], and the close proximity of the cysteine residues at positions 182 and 189 suggests the possibility of disulphide shuffling in this region, facilitating cross-linking of monomers. We assessed this directly by mutating Cys-203 to serine to create hGHDAF28-C203S.

On expression in CHO cells we observed that hGHDAF28-C203S was less rapidly lost than the other constructs tested, but not dramatically so (Figure 4). This suggested that either the fusion protein was a poor ERAD substrate, but was still retained, or that its fate was substantially altered. This latter possibility was shown to be correct when we assessed the location of the fusion protein. In stark contrast to hGHDAF28, hGHDAF28-C203S was found to be secreted from the cell surface.

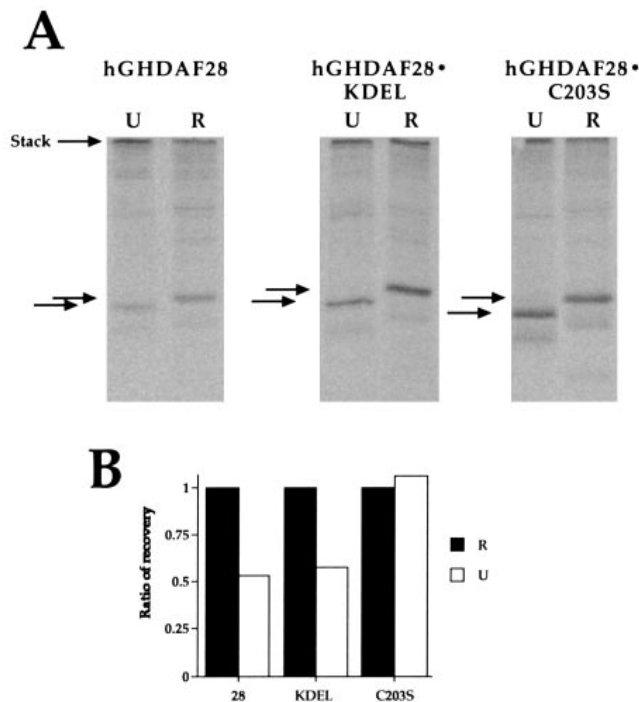


Figure 6 Cys-203 is essential for formation of hGHDAF28 aggregates

SDS/PAGE analysis of immunoprecipitates of hGHDAF28, hGHDAF28·KDEL and hGHDAF28·C203S. Equal aliquots of the same immunoprecipitate were electrophoresed under reducing (lanes R) or non-reducing (lanes U) conditions. **(A)** Composite autoradiogram showing the positions of the hGHDAF28 constructs and their intensities. Arrows indicate migration positions of reduced (upper) and non-reduced (lower) monomeric forms of hGHDAF28. Previous studies indicate that ~50% of hGHDAF28 is recovered in cell lysates as part of disulphide-linked high-molecular-mass complexes and therefore does not migrate with the monomer band [32]. Note that reduced and non-reduced samples were electrophoresed with a free lane to separate them and to prevent diffusion of DTT into the non-reduced lanes. Gel images were reconstructed using Adobe Photoshop 3.01 to place corresponding lanes adjacent and to facilitate easier comparison. **(B)** Quantification of the intensities of the monomer bands in **(A)** by densitometry. The intensity of the reduced band in each case has been set at 1.00. Note that for hGHDAF28 and hGHDAF28·KDEL, significantly more antigen is recovered after reduction, whereas for hGHDAF28·C203S no change is seen. Accuracy of the analysis is $\pm 10\%$. This is a representative experiment of three.

AF28·R4, hGHDAF28·KDEL and hGHDAF29, ~60% hGHDAF28·C203S was recovered efficiently from the medium after 3 h (Figure 5). A small amount of hGHDAF29 was also found in the medium, but is probably due to shedding of this GPI-anchored protein from the cell surface. These experiments suggest that the presence of an unpaired cysteine within the GPI signal is an essential retention determinant for hGHDAF.

We next investigated whether intracellular hGHDAF28·C203S was able to form aggregates like hGHDAF28. We assessed this by comparison of the level of radioactivity recovered in the respective monomer bands before and after reduction with DTT (Figure 6). Previously we have shown that ~50% of hGHDAF28 is incorporated into higher order disulphide-linked species [32] and therefore is not recoverable as monomer without reduction. On reduction, all of the fusion protein is found as the monomer.

We performed this analysis in transiently transfected COS cells by metabolic labelling, immunoprecipitation and SDS/PAGE to resolve the hGHDAF28 band (Figure 6A). Equal aliquots of immunoprecipitate were loaded before and after reduction and

the monomer bands were quantified (Figure 6B). hGHDAF28 behaved as expected, with approximately 50% of the protein present as an aggregate. Owing to reduction of the two disulphide bridges in the hGH domain, which increases the Stokes radius of the protein, the reduced form of hGHDAF28 is found to have decreased mobility in this gel system. The same altered migration was observed for all of the hGHDAF28 proteins. Like the parent protein, hGHDAF28·KDEL also formed an aggregate. In contrast, when we looked at the behaviour of hGHDAF28·C203S we found that reduction had no effect on the recovery of radioactivity, indicating that removal of Cys-203 resulted in failure of the protein to form aggregates. In addition, if we treated cells with DTT we observed that secretion of hGHDAF28·C203S was abolished (results not shown [33]). This effect was presumably due to exposure of new thiols by creation of a reducing potential within the ER and indicates that hGHDAF28·C203S is still capable of being retained by the quality control system.

DISCUSSION

The emerging model for ERAD is that retained protein is transported in a retrograde fashion from the ER back to the cytosol [4,5], probably mediated in part by the sec61p pore complex, and is supported by both biochemical and genetic evidence [6,7,16,20]. Once on the cytosolic face of the ER the ERAD substrate protein is then delivered to the proteasome [12,13,15,17,18,21]. This process may involve the ubiquitination machinery, but for some substrates it is not required [22]. Cytosolic chaperones may also be involved [40]. Re-export processes from the ER are quite common and substrates include glycopeptides and oligosaccharides in addition to proteins [8–10] and probably goes some way towards explaining the mode of action of a number of plant and bacterial toxins.

Here we show that the model GPI-anchored protein, hGHDAF, is also a substrate for this pathway (Figure 7). Our data indicate that the major protease involved in the degradation of hGHDAF28 is lactacystin- and ALLN-sensitive and therefore proteasomal. Uniquely, we also see a lactacystin-resistant proteolytic event, which removes ~2 kDa from the hGHDAF28 molecule. Since this cleavage is unaffected by the additional presence of ALLN, ALLM, antipain or pepstatin, it is unlikely to be mediated by either aspartic, serine or cysteine proteases. We do not know the location of the cleavage generating p24, but as the hGH portion of hGHDAF28 is compact and protease resistant ([41]; L. J. Wainwright and M. C. Field, unpublished work), it is most likely that the C-terminus is the site of the cut. This would remove the majority of the GPI signal, which is implicated as important in cross-linking and retaining the protein. Thus conversion into p24 may be a prerequisite for further handling of the protein ([32] and see below). hGH itself would be expected to be secreted if it were to be released from hGHDAF28 by proteolysis, but in the presence of lactacystin we find that the sum of the intact hGHDAF28 and p24 recovered from cell lysates remains unchanged, indicating that p24 cannot be secreted and therefore suggests that the cleavage producing p24 occurs after association with the ERAD re-export system or is derived from disulphide-linked aggregated material. As none of the non-proteasomal protease inhibitors was effective in preventing the turnover of hGHDAF28 we cannot assign the nature of the activity responsible for this processing event or determine if the step mediated by this activity is essential. It is formally possible that conversion of hGHDAF28 into p24 is only of significance to the lactacystin-treated cell, but in such cells our analysis indicates that the majority of hGHDAF28 passes

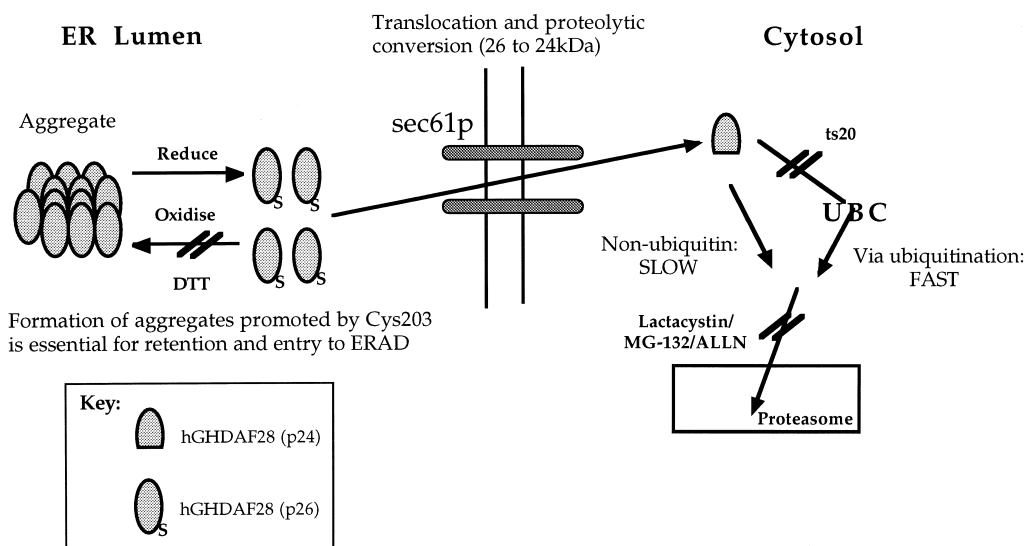


Figure 7 Model for the degradative pathway of hGHDAF28

The scheme is based on the work described in this paper and in [32,33] and current models of ERAD [4]. Steps that are affected by pharmacological or other treatments are indicated by double bars thus //. We propose that after import to the ER, hGHDAF28 rapidly assembles into a mixture of aggregate and monomer [32], which is in equilibrium. The aggregate form cannot be secreted due to size, whereas the monomer is retained by a mechanism related to 'thiol-mediated retention' [38]. The presence of three Cys residues near the C-terminus of hGHDAF28 allows some shuffling and cross-linking to take place within the aggregate. Only the monomeric form can be re-exported from the ER, via sec61p, and therefore addition of DTT to cells, inhibiting thiol oxidation, promotes export and hence a decreased half-life [33]. During export, or at some point thereafter, there is proteolytic removal of a 2 kDa fragment by an ALLN- and lactacystin-resistant protease. Following this, hGHDAF28 is ubiquitinated and rapidly delivered to the proteasome. In the absence of E1 activity, a non-ubiquitin-dependent mechanism delivers hGHDAF28 to the proteasome, by a slow route.

through the p24 form during disposal. Also, the kinetics of production of p24 are similar to those of hGHDAF28 degradation in uninhibited cells, consistent with p24 being a *bona fide* intermediate. However, additional data are required to confirm this, as is the mechanism by which p24 is derived from hGHDAF28.

We also found that hGHDAF28 degradation was accelerated by a functional ubiquitination system, using the well-characterized ts20 temperature-sensitive ubiquitin-deficient cell line [14]. However, the effect was not complete, as we observed reduced but significant degradation at the non-permissive temperature. This could reflect the redundancy of the ubiquitination system, leakiness of the mutant phenotype, or the presence of both ubiquitin-dependent and independent routes. The latter possibility has been clearly demonstrated for the T-cell receptor α -subunit by removal of lysine residues, preventing ubiquitin conjugation [22]. However, from our analysis it is clear that the ubiquitin system does serve to accelerate the rate at which hGHDAF28 is degraded, but we cannot conclude that it is an essential component. We suggest rather that ubiquitin-conjugation represents a fast-track process.

Analysis of the GPI signal by mutagenesis revealed an unexpected finding. Initially we were interested in whether the presence of a KDEL motif would stabilize the fusion protein by interaction with the erd2 receptor. This was found not to be the case. These data firmly rule out transport beyond the ER by normal anterograde vesicle pathways playing a role in the disposal of hGHDAF28 and are consistent with the failure to include non-processed GPI-signal proteins in ER transport vesicles in yeast [30]. In addition, these data indicate that the presence of a small polar region, R4 or KDEL, at the C-terminus of the GPI-signal is not sufficient to destroy the retention properties of the DAF sequence. We also conclude from these

data that the presence of these small polar regions at the C-termini of the fusion proteins is unlikely to have converted them into transmembrane proteins, as these are predicted to be exported to the cell surface.

When we altered the cysteine residue in the DAF28 signal to serine we found a dramatic effect. hGHDAF28·C203S protein was efficiently secreted from the cell and did not appear to enter the ERAD pathway, nor was the protein incorporated into disulphide-linked aggregates. This observation suggests that whereas the presence of the DAF GPI-signal is sufficient for retention it is critically dependent on the presence of Cys-203. Additionally, retention and aggregate formation are found to correlate. At first sight this appears to conflict with observations that most GPI-anchored proteins that fail to be processed are retained and that only a minority of GPI signals contain a cysteine residue [26,31]. However, study of *Trypanosoma cruzi* that over express GPI phospholipase C, resulting in GPI-deficiency, demonstrated that GPI proteins had divergent cellular fates and could either be retained for degradation or secreted [42]. In addition, the presence of a cysteine residue, either in the GPI-signal (e.g. *Dictyostellium* PsA) or very close to it (e.g. Thy-1 or placental alkaline phosphatase, see [43]), suggests that this may not be a unique mechanism. Furthermore, studies with immunoglobulin subunits, specifically λ and μ chains, have also shown the vital importance of a C-terminal unpaired cysteine for retention [38,39], which has led to the suggestion of a 'thiol-mediated retention' system. Our previous experiments using DTT to perturb ER redox led to a decrease in stability for hGHDAF28 [33] and would be consistent with this model (Figure 7). Indeed, DTT treatment also prevented export of hGHDAF28·C203S, consistent with efficient recognition of this class of protein by the 'thiol-mediated' retention system.

Most importantly, our data indicate that hGHDAF28 may

contain two retention motifs, both of which contribute to blocking of efficient secretion: firstly, the GPI signal, which in at least this case is insufficient for full retentive behaviour, and secondly, an unpaired cysteine. This latter is also not always sufficient to prevent secretion of mal-folded or mis-assembled proteins, as oxidized μ -chains can escape the ER [44]. We propose that aggregate formation serves to prevent oxidized hGHDAF28 from escaping the ER, whereas recognition of the unpaired thiol causes retention of the monomeric form. Overall, these observations suggest that the simplistic view, that functional GPI signals are always capable of mediating efficient retention, may be incorrect and that a more complex requirement may be present. Detailed analysis of additional GPI-signal sequences will be necessary to determine the precise requirements. Also, the GPI signal used in the hGHDAF constructs here is a truncated version of the natural DAF sequence [36] and the additional amino acids in the true DAF tail may substitute for the requirement for the unpaired cysteine.

In conclusion, we have demonstrated two important findings in this paper. Firstly, disposal of non-processed GPI-anchored proteins is by the ERAD pathway and involves re-export of the protein to the cytoplasm for proteasomal processing. Secondly, we have shown that the presence of a cysteine residue in the hGHDAF28 GPI-signal is an essential retention determinant for this protein.

We are most grateful to Dr Ger Strous (University of Utrecht, The Netherlands) for the ts20 and E36 cell lines and we thank Dr. Bassam Ali and Dr. Helen Field for comments on the manuscript. The financial support of the MRC (Project grant #9406852 to M.C.F.) is gratefully acknowledged.

REFERENCES

- Hurtley, S. M. and Helenius, A. (1989) *Annu. Rev. Cell Biol.* **5**, 277–307
- Bonifacino, J. S. and Lippincott-Schwartz, J. (1991) *Curr. Opin. Cell Biol.* **3**, 592–600
- Fra, A. and Sitia, R. (1993) *Subcell. Biochem.* **21**, 143–168
- Kopito, R. R. (1997) *Cell* **88**, 427–430
- Brodsky, J. L. and McCracken, A. A. (1997) *Trends Cell Biol.* **7**, 151–155
- Piemper, R. K., Bohmler, S., Boddallo, J., Sommer, T. and Wolf, D. H. (1997) *Nature (London)* **388**, 891–895
- Pilon, M., Schekman, R. and Romisch, K. (1997) *EMBO J.* **16**, 4540–4548
- Romisch, K. and Schekman, R. (1992) *Proc. Natl. Acad. Sci. U.S.A.* **89**, 7227–7231
- Romisch, K. and Ali, B. R. S. (1997) *Proc. Natl. Acad. Sci. U.S.A.* **94**, 6730–6734
- Moore, S. E. H., Bauvy, C. and Codogno, P. (1995) *EMBO J.* **14**, 6034–6042
- McCracken, A. and Brodsky, J. (1996) *J. Cell Biol.* **132**, 291–298
- Werner, E. D., Brodsky, J. L. and McCracken, A. A. (1996) *Proc. Natl. Acad. Sci. U.S.A.* **93**, 13797–13801
- Hiller, M., Finger, A., Schweiger, M. and Wolf, D. (1996) *Science* **273**, 1725–1728
- Strous, G., Kerkhof, P., Govers, R., Ciechanover, A. and Schwartz, A. (1996) *EMBO J.* **15**, 3806–3812
- Ward, C. L., Omura, S. and Kopito, R. (1995) *Cell* **83**, 121–127
- Wiertz, E., Jones, T., Sun, L., Bogoy, M., Geuze, H. and Ploegh, H. (1996) *Cell* **84**, 769–779
- Qu, D., Teckman, J. H., Omura, S. and Perlmutter, D. H. (1996) *J. Biol. Chem.* **271**, 22791–22795
- Craiu, A., Gaczynska, M., Akopian, T., Gramm, C. F., Fenteany, G., Goldberg, A. L. and Rock, K. L. (1997) *J. Biol. Chem.* **272**, 13437–13445
- Dick, L. R., Cruikshank, A. S., Destree, A. T., Grenier, L., McCormack, T. A., Melandri, F. D., Nunes, S. L., Palombella, V. J., Parent, L. A., Plamondon, L. and Stein, R. L. (1997) *J. Biol. Chem.* **272**, 182–188
- Wiertz, E., Torterella, D., Bogoy, M., Yu, J., Mothes, W., Jones, T., Rapoport, T. and Ploegh, H. (1996) *Nature (London)* **384**, 432–438
- Hughes, E. A., Hammond, C. and Cresswell, P. (1997) *Proc. Natl. Acad. Sci. U.S.A.* **94**, 1896–1901
- Yu, H., Kaung, G., Kobayashi, S. and Kopito, R. R. (1997) *J. Biol. Chem.* **272**, 20800–20804
- Field, M. and Menon, A. (1993) in *CRC Handbook of Lipid Modifications of Proteins* (Schlesinger, M., ed.), pp. 83–134, CRC Press, Boca Raton, FL
- Udenfriend, S. and Kodukula, K. (1995) *Annu. Rev. Biochem.* **64**, 563–591
- Caras, I. W., Weddell, G. and Williams, S. R. (1989) *J. Cell Biol.* **108**, 1387–1396
- Gerber, L., Kodukula, K. and Udenfriend, S. (1992) *J. Biol. Chem.* **267**, 12168–12173
- Lippincott-Schwartz, J., Bonifacino, J., Yuan, Y. and Klausner, R. (1988) *Cell* **54**, 209–220
- Oda, K., Ikehara, Y. and Omura, S. (1996) *Biochem. Biophys. Res. Commun.* **219**, 800–805
- Moran, P. and Caras, I. (1991) *J. Cell Biol.* **119**, 329–336
- Doering, T. and Schekman, R. (1996) *EMBO J.* **15**, 182–191
- Delahunty, M. D., Stafford, F. J., Yuan, L. C., Shaz, D. and Bonifacino, J. S. (1993) *J. Biol. Chem.* **268**, 12017–12027
- Field, M. C., Moran, P., Lee, W., Keller, G. and Caras, I. (1994) *J. Biol. Chem.* **269**, 10830–10837
- Wainwright, L. J. and Field, M. C. (1997) *Biochem. J.* **321**, 655–664
- Liang, P. and Pardee, A. B. (1994) in *Current Protocols in Molecular Biology* (Ausubel, F. M., Brent, R., Kingston, R. E., Moore, D. D., Seidman, J. G., Smith, J. A. and Struhl, K., eds.), pp. 15.0.1–15.8.8, Wiley Interscience, New York
- Rock, K. L., Gramm, C., Rothstein, L., Clark, K., Stein, R., Dick, L., Hwang, D. and Goldberg, A. L. (1994) *Cell* **78**, 761–771
- Moran, P., Raab, H., Kohr, W. and Caras, I. (1991) *J. Biol. Chem.* **266**, 1250–1257
- Jackson, M. R., Nilsson, T. and Peterson, P. A. (1993) *J. Cell Biol.* **121**, 317–333
- Valetti, C. and Sitia, R. (1994) *Mol. Biol. Cell* **5**, 1311–1324
- Reddy, P., Sparvoli, A., Fagioli, C., Fassina, G. and Sitia, R. (1996) *EMBO J.* **15**, 2077–2085
- Bercovich, B., Stancovski, I., Mayer, A., Blumenfeld, N., Laszlo, A., Schwartz, A. L. and Ciechanover, A. (1997) *J. Biol. Chem.* **272**, 9002–9010
- deVos, A. M., Ulsch, M. and Kossiakoff, A. A. (1992) *Science* **255**, 306–312
- Garg, N., Terleton, R. L. and Mensa-Wilmot, K. (1997) *J. Biol. Chem.* **272**, 12482–12491
- Cross, G. A. M. (1990) *Annu. Rev. Cell Biol.* **6**, 1–39
- Brewer, J. W. and Corley, R. B. (1996) *J. Cell Sci.* **109**, 2383–2392